Research Article Open Access

Khuram Shahzad Ahmad*, Shaan Bibi Jaffri

പ്പ

Phytosynthetic Ag doped ZnO nanoparticles: Semiconducting green remediators

Photocatalytic and antimicrobial potential of green nanoparticles

https://doi.org/10.1515/chem-2018-0060 received November 10, 2017; accepted April 3, 2018.

Abstract: Highly stable semiconducting silver doped zinc oxide nanoparticles have been synthesized via facile, biomimetic and sustainable route, through utilization of Zinc acetate dihydrate (C,H,O,Zn · 2H,O) as host, Silver nitrate (AgNO₃) as dopant and phytochemicals of angiospermic medicinal plant Prunus cerasifera as the reducing agents. Synthesis of Ag doped ZnO nanoparticles was done in a one pot synthetic mode by varying the amount of dopant from 0.2 - 2.0%. Synthesized photocatalyst nanoparticles were analyzed via UV-vis, FTIR, XRD and SEM. Commendable alleviation in the direct band gap i.e. 2.81 eV was achieved as a result of doping. Silver doped zinc oxide nanoparticles size ranged between 72.11 - 100 nm with rough surface morphology and higher polydispersity degree. The XRD patterns revealed the hexagonal wurtzite geometry of crystals with an average crystallite size of 2.99 nm. Persistent organic dyes Methyl Orange, Safranin O and Rhodamine B were sustainably photodegraded in direct solar irradiance with remarkable degradation percentages up to 81.76, 74.11 and 85.52% in limited time with pseudo first order reaction kinetics (R^2 =0.99, 0.99 and 0.97). Furthermore, efficient inhibition against nine microbes of biomedical and agriculturally significance was achieved. Synthesized nanoparticles are potential green remediators of polluted water and perilous pathogens.

1 Introduction

Metallic oxide nanoparticle have been known for their mesmerizing applications in different domains of electronics, energy storage devices, ecological remediation, microbe inhibition, medical implants and optical appliances. Thus, the synthesis and engineering of metallic oxide nanoparticles finds great scope [1] in present era of urbanization and industrialization. For environmental remediation in a sustainable manner, metal oxides are of prime importance. Water decontamination has been explored with variety of metal oxides and results were suggestive of that all metallic oxide nanoparticles, Zinc oxide (ZnO) has tremendous potential for photo catalysis by the virtue of its stable nature in exposure to light due to larger band gap of 3.37 eV, augmented efficiency and lower cost. ZnO has been utilized on industrial scale for wurtzite structural conformation and semiconducting attributes [2]. ZnO is found to surpass TiO₃ in water remediation due to generation of ROS (radical oxygen species) subsequently executing remarkable mineralization outputs, as well as increased reaction sites due to higher surface reactivity. ZnO has been found to produce rapid reaction rates in terms of photocatalysis due to presence of highly active sites with an elevated surficial reactivity [3]. ZnO has been known as one of the representative semi-conductor having negligible cost, availability and eco-compatibility. Significant characteristics physicochemical characteristics associated with ZnO nanoparticles has attracted researchers to further explore the electronic, photocatalytic and sensing applications. ZnO nanoparticle chemical sensitization in electronic perspective has been achieved by doping with noble metals or metal ions, n- or p- type loading of other

Shaan Bibi Jaffri: Department of Environmental Sciences, Fatima Jinnah Women University, The Mall, 46000, Rawalpindi, Pakistan

Keywords: *Prunus cerasifera*; doping; characterization; photocatalysis; antibacterial; antifungal.

^{*}Corresponding author: Khuram Shahzad Ahmad, Department of Environmental Sciences, Fatima Jinnah Women University, The Mall, 46000, Rawalpindi, Pakistan, E-mail: chemist.phd33@yahoo.com; chemist.phd33@fjwu.edu.pk

substances with inherent semi conducting properties [4]. Nanostructured ZnO loaded with metallic ions is done for enhancement in its chemical and mechanical peculiarities i.e. catalysis, semi conduction, magnetism, thermal, optical and electric response. Such doping also influences the ZnO nanoparticle size range, crystal dimensions and increases the surface to volume ratio [5, 6]. Ag is considered as one of the best options in selection of dopant for its potential in generation of electrical field and subsequent improvement in galvanic attributed due to SPR (surface plasmon resonance) [7]. Despite such commendable results, reports available on Ag doped ZnO nanoparticles are scanty, thus opening a new arena of scientific investigation regarding impact of Ag doping in ZnO nanoparticles. Ag doped ZnO nanoparticles are expected to be used enormously for their novel physicochemical and geometrical properties since Ag doping in ZnO is associated with induction of oxygen vacancies [8], crystalline transformation [9] and alterations in light scattering patterns.

Ag doped ZnO nanoparticles have been fabricated by variety of physicochemical processes e.g. sol-gel, oxidative reactions, thermo- evaporative, co- precipitative, vapor deposition through chemical method and sonochemical reactions. These all processes are associated with utilization of chemicals causing harm to environment or requiring complication operative conditions. Green chemistry demystified the biogenic route for Ag doping in ZnO nanoparticles by utilization of phytochemicals from plants. Despite such exceedingly higher transformation induced by doping, studies focused on biogenic synthesis of Ag doped ZnO nanoparticle are scarce. Ag as well as ZnO nanoparticles have been fabricated with variety of plants [10-15] yet none reported the doping of Ag doping into ZnO nanoparticles by biogenic route. Prunus cerasifera, a medicinal plant with reservoir of antioxidant compounds is not only used for pharmacological purposes but also for preparation of wine, jams, marmalades due to its pleasant taste and widespread occurrence in Asian and some European regions, has great potential to be used in biogenic synthesis. P. cerasifera is also known as cherry plum belonging to family Rosaceae, Prunoideae, and Prumus. This plant is not only found in wild but is also cultivated due to its rapid growth, appreciable adaptiveness and rich phytochemical resource. Currently, P. cerasifera has been explored in terms of landscaping and molecular characterization, however no reports are available on utilization of it in greener synthesis of metallic oxide nanoparticles. Thus fact makes it a potential candidate to be investigated for biogenic synthesis.

Environmental deterioration resulting from industrial effluents comprising dye materials in form organic contaminants has been prevalent since many decades. Around 1-20% of dyes during manufacturing processes are released to environment in form of effluents. Such release is associated with metabolites formation from partial biodegradation. These metabolites are not only toxic but also carcinogenic and mutagenic in nature hindering the normal functioning of aquatic flora and fauna [16] Successful environmental remediation of such recalcitrant dves lies in their treatment prior to their dumping in wastewaters. Though variety of physicochemical and biological treatment modes have been devised in this regard, but economical and practical considerations have rendered them difficult in adaptation. Thus, utilization of nanomaterials for pollutant degradation in a photocatalytic oxidative pathway through mineralization has been found to be economical, rapid and efficient in comparison to conventional methods [17]. Currently efforts are being done for transformation of ZnO by addition of metallic impurities e.g. Ag, Au and Pt etc. for scavenging the photogenerated electrons enhancing the electron-hole disjunction and increasing the photonic charges for an elevated photocatalytic performance [18]. In this regard, silver has been specially doped into ZnO nanoparticles and commendable photocatalytic activity is obtained [19, 20]. Ag doped ZnO nanoparticles have been extensively studied for their photocatalytic potential in degradation of persistent dyes e.g. Methylene Blue, Brilliant blue, Methylene orange, Napthol blue black, Rhodamine etc. [21-25]. Ag doped ZnO in a photocatalytic reaction are found to be effective in lower photonic energy due to electronic excitation. Ag as a dopant accepts the electrons by trapping electrons from conduction band of ZnO [26, 27] causing an augmentation in photocatalytic activity by inhibition of electron-hole re-joining [28]. Photocatalytic activity against various dyestuff pollutants has been found to be more effective with Ag doped ZnO than pure ZnO nanoparticles [29-31].

Microbial strains including bacteria and fungi have expressed remarkable adaptability towards a wide range of antibiotics exhibiting multidrug resistant (MDR). Such resistance of pathogenic microbes towards inhibitory substances is not only alarming for human beings but also for agricultural sector prone to pathogenic attacks [32]. In this regard, nanoparticles having an alleviated sizes and defined morphologies have been found as an effective solution in combating microbial pathogens. Ag, ZnO and Ag doped ZnO nanoparticles have been reported to be an effective antibacterial and antifungal agents [33] against a variety of microbes e.g. Staphylococcus

epidermidis expressed sensitivity towards Ag doped ZnO nanoparticles synthesized via hydrothermal route [34]. In case of Ag doped ZnO nanoparticles, the antimicrobial activity was found to be dependent upon size, shape as well as the Ag dopant loading amount. Several pathogens have been inhibited by Ag doped ZnO nanoparticles in an exceedingly remarkable activity in comparison to standard antibiotic drugs. Such an achievement is suggestive of developing Ag doped ZnO into commercial scale bactericide. The augmented antimicrobial activity carried out in direct solar irradiance of Ag doped ZnO nanoparticles can be attributed to the photo activation of Ag and ZnO. Hence, Ag doped ZnO nanoparticles are potential candidates for development into economical and commercially ascendable antimicrobial product against pathogenic microbes [35]. Ag doped ZnO nanoparticles causes the disruption of nucleic acids and protein linkages in microbial cells and thus killing the cell. Such nanoparticles have been effectively used against variety of microbes particularly in waste water treatment for bacterial inhibition [36]. Though some investigations have supported the enhanced antimicrobial activity of pure ZnO nanoparticles in comparison to doped ones but [37], however majority of results have expressed the superior activity of doped ZnO nanoparticles [38-40]. Increment in Ag dopant concentration gives rise to higher antimicrobial activity due to availability of Ag+ followed by ZnO in generation of hydrogen peroxide. Thus Ag and ZnO working in synergistic manner gives an amplified inhibitory activity interfering with the enzymatic assemblage of respiratory chain and annihilating DNA formation [41].

In this study, Ag nanoparticles were doped into ZnO nanoparticles via facile and biomimetic route of using the phytoconstituents from P. cerasifera fruit as a substitution of chemical reducing agents. Methods adopted were in complete conformity with principles of Green chemistry employing biological medium instead of environmentally toxic reducing agents. Doping concentration was varied from 0.2 – 2.0 % by weight percent of the dopant Ag. Optical, structural and morphological attributes of biogenic silver doped ZnO nanoparticles (BSDZNPs) were analyzed via Ultraviolet spectroscopy (UV-vis), Fourier Transform Infrared analysis (FTIR), X-ray powder diffraction (XRD) and Scanning electron microscopy (SEM) and band gap was calculated by Tauc plot. Furthermore, the photo catalysis potential of semiconducting BSDZNPs was evaluated for remediation of persistent environmental pollutants i.e. Methyl Orange (MO), Safranin O (SO) and Rhodamine B (RB) in direct solar irradiance. The inherent antimicrobial activity possessed by Ag dopant and ZnO nanoparticles was also assessed for inhibition of pathogenic strains having known toxicity towards humans and agricultural crops. BSDZNPs synthesized from P. cerasifera fruit extract were checked against two bacterial and seven fungal strains i.e. X. citri, P. syringae, A. niger, A. flavus, A. fumigatus, A. terreus, P. chrysogenum, F. solani and L. theobromae. Augmented photocatalytic activity of BSDZNPs makes them potential candidate as a water remediation in addition to their nano bacterial and nano fungicidal property against pathogens. Current study strongly supports the large scale industrial development of BSDZNPs into water remediators and new generation antimicrobial agent.

2 Experimental

2.1 Materials

Silver nitrate (AgNO₃), Zinc acetate dihydrate (C₄H₆O₄Zn · 2H₂O), Potassium bromide (KBr) and nutrient agar (NA) culture media were purchased from Merck, Germany. Dves were purchased from BDH, England. Potato dextrose agar (PDA) culture media was purchased Liofilchem, Italy. All chemicals used in investigation were of analytical grade and have been used without further purification.

2.2 Fruit extract preparation

P. cerasifera ripened fruits collected from Ali Zai area of Parachinar, Pakistan in July, 2016. They were ground into fine powder with help of pestle and mortar, sieved and stored in sealed polyethene bags. For aqueous filtrate preparation, 10 g of fruit powder was weighed and extracted with 1000 mL deionized water and heated at 30°C for 10 min. It was followed by double filtration with Whatman No. 1 filter paper (pore size: 11µm) and refrigerated at 4°C for further use (Figure 1a-e). Prior to synthesis, the fruit extract was centrifuged at 2500 rpm for 10 min for getting clear solution of *P. cerasifera*.

2.3 Synthesis of BSDZNPs

Zinc acetate dihydrate (C,H,O,Zn · 2H,O) was used as ZnO source by dissolution of 5 g in 50 mL of deionized water at room temperature, Silver nitrate (AgNO₂) was used as the dopant source by taking variable weight percentages from 0.2 – 2.0% and P.cerasifera fruit extract (PCFE) was used as a reducing cum stabilizing agent for BSDZNPs. 2



Figure 1: P. cerasifera (a) unripe fruit May, 2016; (b) ripened fruit July, 2016; (c) dried fruit; (d) fruit powder for extract preparation; (e) fruit extract.

mL of aqueous solution of AgNO, was added into C, H, O, Zn · 2H₂O solution with addition of 5 mL of *P.cerasifera* fruit extract in drop wise manner with constant stirring with glass rod. Assembly of eleven beakers with different concentrations of dopant i.e. 0.2, 0.4, 0.6, 0.8, 1.0, 1.2, 1.3, 1.4, 1.6. 1.8, 2.0% were irradiated by direct sunlight for 20 minutes. Direct solar exposure triggered the formation of precipitate which were collected and washed twice with ethanol for removal of unreacted P.cerasifera fruit phytoconstituents. Precipitate were dried at 100 in hot air drier (UN110, Memmert, Germany) for 2 hours followed by drying at 400 in BSDZNPs furnace (D550, Ney Vulcan, USA) for 2 hours at air atmospheric conditions [42]. White colored final product was ground into fine powder and used for characterization and applications.

2.4 Characterization

BSDZNPs were analyzed via UV-Vis Spectrophotometer (1602, Biomedical services, Spain) in range of 200-800nm. The measurement of UV-Vis spectrum was done by preparation of BSDZNPs homogenous suspension in double distilled water. Homogenization in this case was achieved by ultra-sonication for 25 min. The interplay of such functional groups was checked by FTIR Spectrophotometer (8400, Shimadzu, Japan). Pellet was prepared for FTIR analysis by preparing a homogenous mixture of BSDZNPs powder with KBr (1:3) for complete moisture removal. The pellet was exerted upon a pressure of 5 tons with help of pellet forming die. Prepared pellet was analysed at ambient conditions. Surface morphology and particle size ranges were analyzed by scanning electron microscopy (SEM JOEL JSM-6490, Germany) by gold coating on sputter coater and observed. Crystalline properties of BSDZNPs were analysed by XRD patterns, recorded with Bruker AXS D-8 powder X-ray diffractometer (Shimadzu, Japan), operated at 40 kV, 20mA, with CuKa radiation ($\lambda = 1.5406 \text{ Å}$).

2.5 Photocatalytic dye degradation (PDD)

Finely powdered BSDZNPs having white colour were utilized for photocatalytic dye degradation. Semiconducting BSDZNPs photocatalytic activity was checked for Methyl Orange, Safranin O and Rhodamine B in two sets comprising of first set where the absorbance of dye solution without NP addition was checked and it was kept in sunlight for 60 min from 12:00-1:00 PM on a sunny day with an average intensity 68-73 Klux (LT300, Extech, UK). The second set of dyes was mixed with BSDZNPs solution and was kept under same conditions. Photocatalytic degradation (second set) comprised of reaction between 250 mL of 20 ppm of each dye solution and 50 mg of BSDZNPs. 250 mL (dye) aqueous solution

and 50 mg BSDZNPs photo catalyst were kept in dark and stirred magnetically for 30 min in quartz beaker for establishment of adsorption and desorption equilibrium. Such adsorptive/desorptive interactions were developed on BSDZNPs photo catalyst surface in mentioned time. After reaction initiation, 5 mL were taken from each set at pre-determined time intervals followed by centrifugation at 6000 rpm for 10 min. Prior to UV-vis analysis, these sets were also exposed to UV-lamp (SN500712, Kohler, Germany) and then spectra were noted from 300-600 nm. Spectra were noted at specific times intervals in addition to the discoloration detected and the values were compared with dves' lambda maximum. PDD percentages were calculated. Degradation was monitored by UV-Vis spectrophotometer and alleviating absorbance was recorded for calculating the rate of reaction and degradation percentages by:

% Degradation =
$$(Ai - Af / Ai) \times 100$$
 (1)

Where A represents the dyes' initial absorbance while A is the dyes' final absorbance after addition of BSDZNPs. Reaction rates were also determined for photocatalytic degradation.

2.6 Antimicrobial assay

Antimicrobial potential of BSDZNPs was tested against nine pathogenic strains i.e. X. citri, P. syringae, A. niger, A. flavus, A. fumigatus, A. terreus, P. chrysogenum, F. solani and L. theobromae by standard Kirby-Bauer disc diffusion assay. Antibacterial and antifungal activity were compared with standard drug Ampicillin and Amphotericin B respectively. Petri plates were autoclaved and stored in oven to avoid contamination, laminar flow hood was decontaminated by cotton swiping with spirit and UV was also turned on for 10min before initiation of experiment. NA and PDA media were autoclaved prior to use. For both assays, the petri plates after completion of working were packed with paraffin tape and shifted to incubator. BSDZNPs' stock solution was prepared by suspension of BSDZNPs in analytical grade CH₂OH for obtaining the final concentration of 100 mg/mL. 30 min sonication with 7 min of repeating cycle was done for BSDZNPs stock solution. Experiments were strictly done within 60-120 min of sonication. BSDZNPs stock suspension was refrigerated at 4 °C with exposure to strenuous vortex mixing before antimicrobial assay. The variable dose inhibition was evaluated by discs loading with 2, 4, 6 and 10 μL of BSDZNPs for both assays.

2.6.1 Antibacterial disc diffusion assay

For antibacterial assay, the bacterial cultures dilution was prepared, followed by autoclaving with 5% saline of final volume was achieved with 105 -106 CFU/mL. CH₂OH diluted BSDZNPs were then loaded onto the properly autoclaved discs and allowed to dry for achievement of complete disc saturation with BSDZNPs. Clean autoclaved discs were placed on pre solidified NA plates and loaded with mentioned BSDZNPs dose. Clean autoclaved discs were also loaded with 10 µL of standard antibacterial drug Ampicillin and 10 µL PCFE as a control. Ampicillin, PCFE and variable dose BSDZNPs dipped discs were meticulously placed on bacterial laws on NA media with 24 h incubation time at 37°C in incubator (Sanyo MR-153, GeminiBV, Netherlands) followed by measurement of zones of inhibition (ZOI) in mm after 24 h.

2.6.2 Antifungal disc diffusion assay

For antifungal activity, fresh fungal mycelia were produced for seven test strains grown on PDA and incubated at 25±1°C for 5 days. Round 0.45 cm discs from the freshly grown mycelial culture were obtained with sterile inoculation needle and inserted at middle of PDA plate. Clean autoclaved discs were also loaded with 10 uL of standard antibacterial drug Amphotericin B and 10 µL PCFE as a control. While experimental set for dose dependent inhibition of BSDZNPs comprised of 2, 4, 6 and 10 µL loaded discs on PDA media with fungal culture of mentioned types. The plates were incubated for 72 h. The zones of inhibition were recorded and compared with standard drug Amphotericin B.

Ethical approval: The conducted research is not related to either human or animals use.

3 Results and discussion

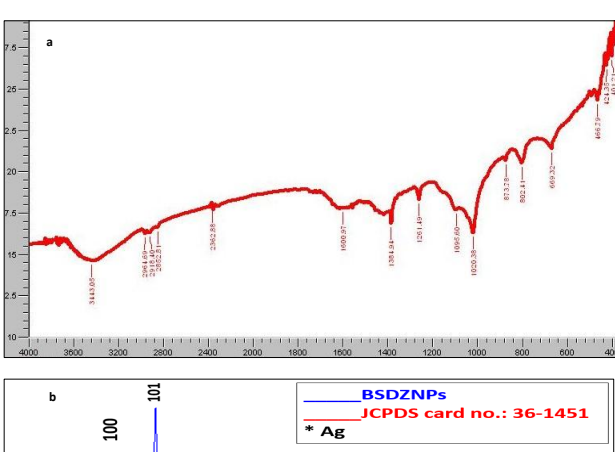
3.1 Characterization of BSDZNPs

3.1.1 FTIR

BSDZNPs synthesized with phytochemicals from P. cerasifera fruit extract were initially confirmed by the formation of precipitates. The dried BSDZNPs were analyzed for presence of functional groups via Fourier Transform Infrared analysis (FTIR). FTIR spectra was recorded between the wavenumber spanning over a range of 4000–

Table 1: Functional groups detected in biogenic silver doped ZnO nanoparticles calcined at 400.

FTIR peaks (cm ⁻¹)	Bond	Assigned functional groups	
3443.05	O-H stretch, H-bonded	Alcohols, Phenols	
2964.05	C-H stretch	Alkanes	
2918.40	C–H stretch	Alkanes	
2852.81	C–H stretch	Alkanes	
1600.97	N-H bend	1° Amines	
1261.49	C-N stretch	Aromatic Amines	
1095.60	C-N stretch	Aliphatic Amines	
1020.38	C-N stretch	Aliphatic Amines	
873.78	C-Cl stretch	Alkyl Halides	
669.32	-C≡C-H: C-H bend	Alkynes	



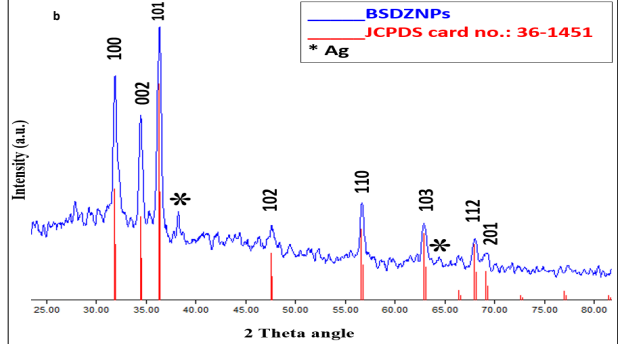


Figure 2: (a) FTIR spectrum for functional groups in biogenic silver doped ZnO nanoparticles (BSDZNPs) calcined at 400; (b) XRD pattern at highest doping concentration i.e. 2.0% for (BSDZNPs).

400 cm⁻¹ (Figure 2a). Various functional groups were detected in BSDZNPs (Table 1) which are possibly derived from P. cerasifera fruit extract playing an influential role in reduction cum stabilization of BSDZNPs. Particularly, 3443.05 cm⁻¹ and 1600.97 cm⁻¹ of O-H stretch and N-H bend are indicative of presence of phenolic components and proteins that are actively involved in bioreduction occurring during doping of Ag onto ZnO nanoparticles. Such functional groups are involved in capping of various plant molecules. Biomolecules develops interactions with metallic salts via functional groups and participates in capping action. Comparatively alleviated intensities were seen due to the capping of these NPs with organic portions of P. cerasifera [43, 44]. Additionally, the broader 3443.05 cm⁻¹ band can be attributed to the water molecules deposited upon BSDZNPs via physio sorption governed by weaker bonding [45]. 873.78 and 669.32 cm⁻¹ bands exhibit weaker absorption region which is the characteristic of metal oxide stretch [46]. Deviation of absorption bands for BSDZNPs in comparison to Ag and ZnO nanoparticles investigated earlier can be due to transformation in bond lengths as a consequence of Ag doping onto ZnO. Such transformation is triggered when partial substitution of cationic silver into ZnO lattice takes place [47]. FTIR spectra for BSDZNPs depicts strong vibrational mode hence indicative of the remarkable doping between host ZnO and dopant Ag material.

3.1.2 XRD

BSDZNPs were investigated for crystallinity by X-ray diffraction analysis. XRD pattern confirmed the presence of different peaks with $2\theta = 31.87^{\circ}$ (100), 34.48° (002), 36.33° (101), 47.56° (102), 62.91° (110), these peaks were consistent with JCPDS card no. 36-1451 (Figure. 2 (b)) for BSDZNPs indicative of hexagonal wurtzite geometry. Extra peaks at 2θ = 38.03° and 64.47° corresponding to (111) and (220) are consistent with JCPDS card no. 89-3722 and exhibits the crystalline nature of Ag NPs with face centered cubic geometry [48, 49]. Highly sharp and intense diffraction peaks expresses the significant crystallinity of BSDZNPs [50]. ZnO hexagonal wurtzite structure is composed of hexagonally arranged oxygen atoms with half tetrahedral sites occupied by zinc atom thus both atoms acquiring equivalent positions [51]. However, no influence of Ag doping onto ZnO has been observed on position of XRD peaks for wurtzite ZnO but it has significantly altered the peak intensities. There is an alleviation in peak intensity broadening upon and increase in Ag doping onto ZnO due to replacement of Ag+ into host ZnO crystal lattice [52]. In addition to this, the diffraction pattern for BSDZNPs doesn't exhibit any peak at 2θ = 32.97 ° thus confirming the absence of Ag₂O in doped product [53]. Absence of any extra peak for plant phytoconstituents or other probable impurities confirms the highly pure nature of BSDZNPs. Furthermore, from successful formation of BSDZNPs confirmed via XRD pattern, it is clear that PCFE phytochemicals play influential role in reduction cum stabilization of the prepared nanoparticles as a green alternative to chemical reducing and capping agents. The average crystallite size obtained from XRD patterns was 2.99 nm calculated from Scherer's equation:

$$D = [K \lambda / \beta \cos \theta] x \mathring{A}$$
 (2)

where, D is representing the average of crystal size in Å, K (0.9) is shape factor, $\lambda(1.5406 \text{ Å})$ is wavelength of X-ray Cu Ka radiation, θ is the Bragg angle and β is the corrected line expressing NPs broadening.

3.1.3 SEM

Morphological features and size ranges for BSDZNPs were analysed by scanning electron microscopy (SEM JOEL JSM-6490, Germany). Variation in dopant percentage not only influenced the shapes of nanoparticles but size reduction was observed with an increase in dopant weight. Rough surface morphologies were exhibited by BSDZNPs (Figure 3a-c) and the three highest dopant concentrations i.e. 1.6%, 1.8% and 2.0% expressed size ranges of 82.46 – 101.98 nm, 72.11 – 128.06 nm and 72.11 – 100nm (Supplementary material Figure 1). SEM images exhibit that synthesized doped nanoparticles were in nano range. Earlier studies have associated such size reduction with calcination temperatures as well [54]. Sizes for BSDZNPs were indicative of order of nanometres thus can be of potential interest for photocatalytic and biomedical applications [55]. BSDZNPs surface morphologies are indicative of close packed organisation of particles and Ag doping caused changes in the shapes of particles. Figure 3 expressed that BSDZNPs comprised of spherical, linear and irregular shaped nanoparticles of varied sizes. The smaller sizes of synthesized nanoparticles signifies the advantage of P. cerasifera fruit extract as a reducing agent in absence of any other chemical agent. The changes detected in morphologies upon varying dopant concentration can also be attributed to the induction of higher number of defects leading to deformation of ZnO lattice structure. There is also a decrease in the agglomeration as a result of higher Ag doping concentration [25].

3.2 Energy band gap

The direct energy band gap for BSDZNPs was also calculated by Tauc plot:

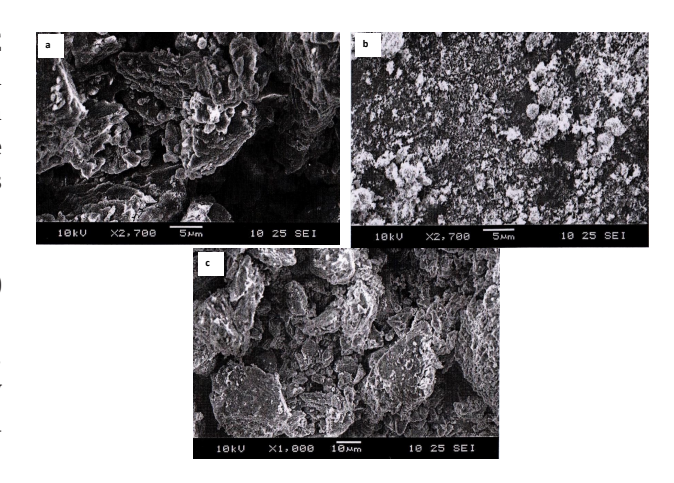


Figure 3: SEM micrographs of biogenic silver doped ZnO nanoparticles (BSDZNPs) (a) 1.6% dopant; (b) 1.8% dopant; (c) 2.0% dopant.

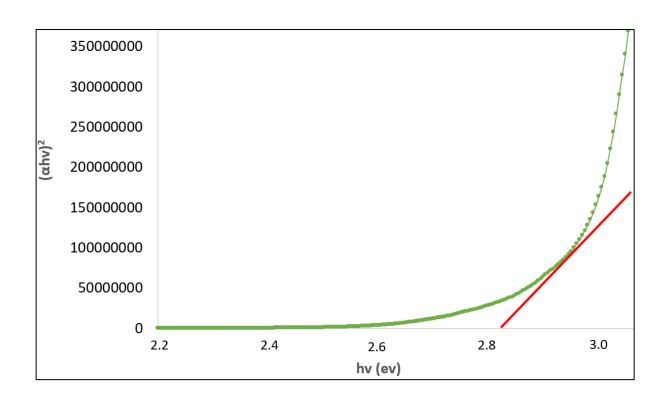


Figure 4: Plot between hv(eV) and $(\alpha hv)^{1/2}$ for direct band gap at highest doping concentration of biogenic silver doped ZnO nanoparticles at highest doped concentration 2.0%.

$$\alpha h v = A (h v - Eg) 1/2$$
 (3)

Where α is absorption coefficient; h is Plank's constant; ν is vibration frequency and $E_{_{\rm g}}$ is band gap. Tauc plot was obtained by plotting hv on X-axis and (αhv) ² on Y-axis. Figure 4 shows the linearity expressing the direct transition of semiconducting BSDZNPs. The extrapolation of this plot gives a band gap of 2.81 eV [51] after doping of Ag onto ZnO nanoparticles thus expressing the potential of BSDZNPs not only as efficient photo catalysts but also their future prospects to be used in solar cell based devices. Such a significant reduction in band gap due to Ag doping in ZnO can be due to vacancy of oxygen which ease the transfer of electrons between valence and conduction band [55, 56]. BSDZNPs were checked for post synthetic stability after 3 months and the results exhibited higher stability at ambient conditions.

Figure 5: Chemical structures of organic dyes (a) Methyl Orange; (b) Safranin O; (c) Rhodamine B.

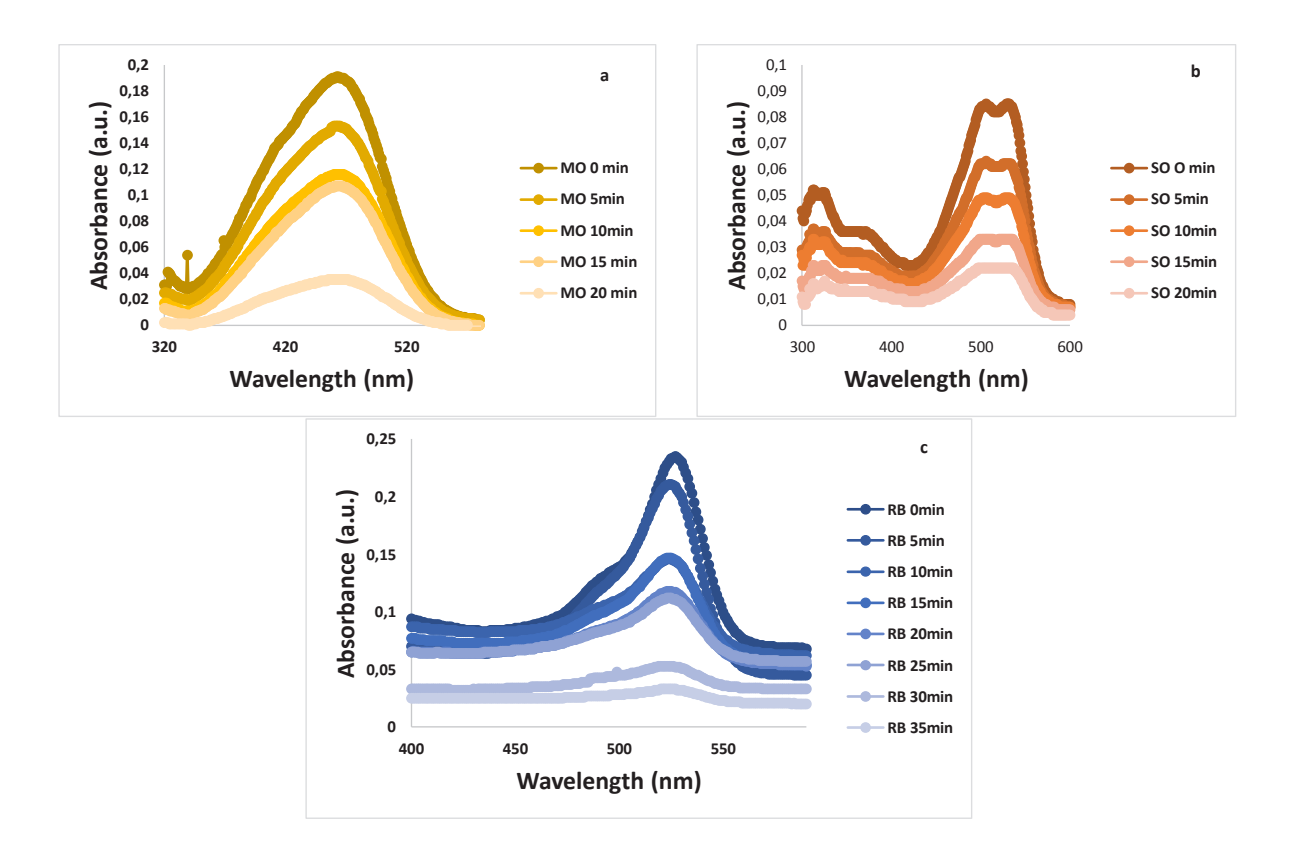


Figure 6: Alleviating UV-vis spectra expressing photocatalytic dye degradation potential of biogenic silver doped ZnO nanoparticles (1.6% doped) (a) Methyl Orange; (b) Safranin O; (c) Rhodamine B.

3.3 Photocatalytic dye degradation

Azo dyes having organic nature usually pose refractoriness and permanence towards different chemical substances, heat and temperature [57, 58]. Efforts have been made for alleviating organic dyes content in sewer waters and natural ecological compartments. The photocatalytic efficiency of BSDZNPs was evaluated for Methyl Orange $(C_{14}H_{14}N_3NaO_3S)$, Safranin O $(C_{20}H_{19}ClN_4)$ and Rhodamine B (C₂₀H₂₁ClN₂O₂) (Figure 5). All photocatalytic experiments were performed with Ag-ZnO (1.6%) since the use of highest doped BSDZNPs may end up acting as a centre for charge concurrence. Such enhanced charge concurrence has been associated with higher Ag loading onto ZnO giving rise to strong attraction between negatively ionic silver and oppositely charged ZnO surface holes [59]. Additionally, at higher doping concentrations, the UV photon utilization of ZnO may be negatively affected thus reducing the overall photocatalytic potential of BSDZNPs [60]. Thus, 1.6% doped BSDZNPs were investigated for photocatalytic reaction. Photocatalytic dye degradation primarily identified by discoloration is an important factor

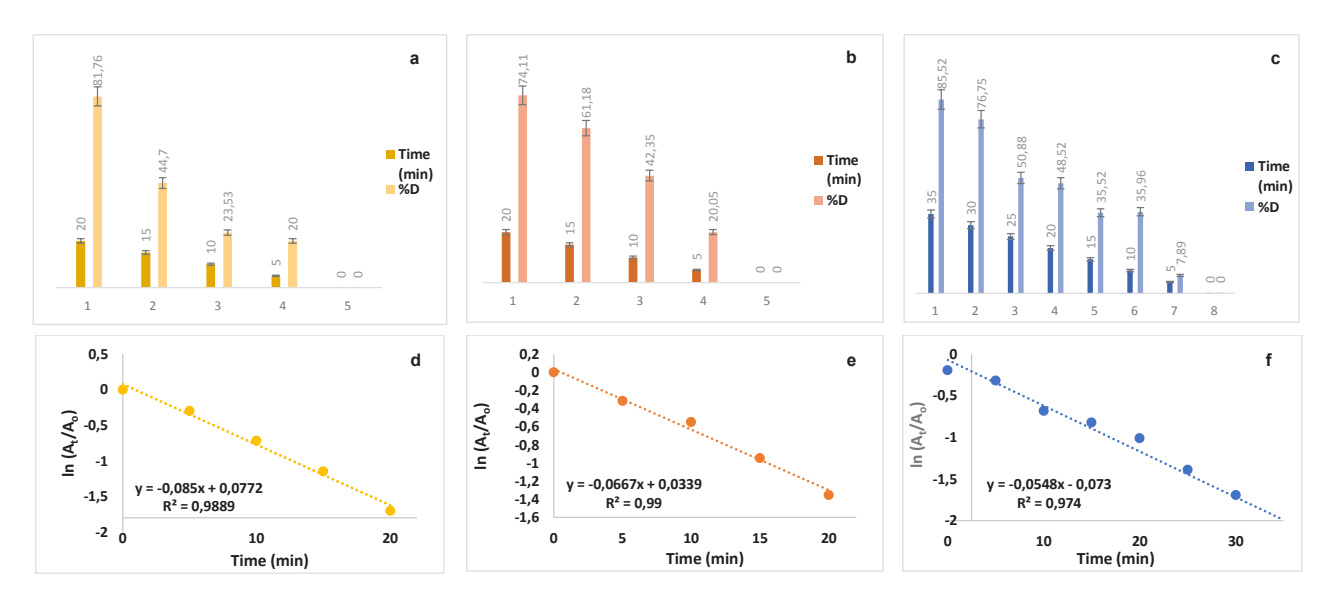


Figure 7: (a,b,c) Percent degradations of Methyl Orange, Safranin O and Rhodamine B for 1.6% doped BSDZNPs; (d,e,f) In (At/Ao) vs time plot of Methyl Orange, Safranin O and Rhodamine B.

in all types of degradation studies [61]. The degradation was initially confirmed by discoloration of the dyes when exposed to direct solar irradiation followed by UV-vis monitoring (Figure 6). However, dye solutions without BSDZNPs addition expressed no changes signifying the role of BSDZNPs in photo catalysis. Thus, the photo induced self-sensitization for tested dyes can be neglected.

Comparison of photocatalytic potential for BSDZNPs for 20 min exhibits the maximum degradation percentage for MO (81.76%) followed by SO (74.11%) and least for RB (48.52%) (Figure 7a-c), however RB was 85.52% degraded in 35 min expressing time dependent photo catalysis of RB. Comparatively longer degradation time for RB can be due to the stronger physio sorption of RB molecules on BSDZNPs catalyst, thus desorption is prolonged. RB, an azo dye is source of producing highly tumorigenic amines of benzene contents through inherent degradative reduction in absence of oxygen [62]. RB is utilized in luminescent docketing [63, 64]. SO, being nonhazardous but can cause optical, respiratory and digestive track ailments upon continuous exposure [65]. Current results for MO [66] and RB [53, 60, 67] are comparable with commercially prepared Ag doped ZnO NPs, but no similar investigation based upon SO degradation with ZnO or doped ZnO NP sare available so far. Such results make phytosynthetic BSDZNPs to be the green alternative to chemically synthesized doped materials. Such photocatalytic performance has been contributed equally by interaction of Ag and ZnO [68].

Photocatalytic reaction kinetics were determined by the plot of ($\ln{(A_t/A_o)}$ vs time). BSDZNPs for MO, SO and RB shown the pseudo first order kinetics with R^2 =0.99, 0.99

and 0.97 respectively [68] (Figure 7d-f). Remarkable band gap reduction from 3.37 to 2.82 eV observed for BSDZNPs has influenced the photo degradation. Reduction in band gap is associated with enhanced visible light absorption and an efficient transference of electrons between excited dye and BSDZNPs through Ag NPs [68, 69]. While, such augmented photocatalytic property has not been reported for semiconductor in pure forms. Undoped semiconductors are marked by reduced performance in terms of sustainability for longer durations, photo degradation disbandment and capacious energy band. Thus doping of ZnO with Ag is highly effective for oxidation and adsorption of dyes than ZnO in isolation [46, 70]. The enhanced optical attributes in addition to high surface to volume ratio caused higher degradation rates. Increased photocatalytic activity of BSDZNPs in a short duration suggests them to be used in remediation of water treatment in cost effective and eco-friendly manner.

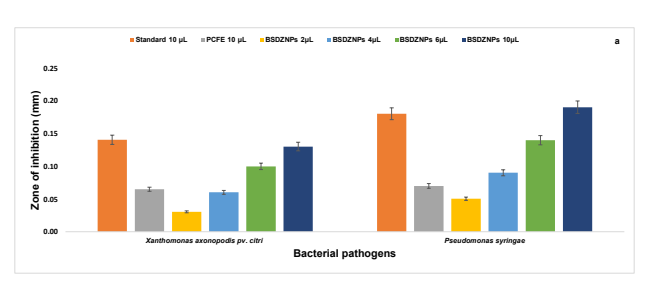
3.4 Antimicrobial activity

Variety of antimicrobial agents available on commercial scale, which were considered miraculous once have now been found ineffective against microbes due to development of drug resistance in them. Drug resistance in microorganisms is a challenge on global scale [71]. Nanotechnology has emerged as a vanquishing field for solving this issue by use of nanoparticles, since resistance to these nanoparticles is less likely because of the requirement for manifold instantaneous genetic

Table 2: In vitro antibacterial and antifungal efficacy of biogenic Ag doped ZnO nanoparticles (highest doped 2.0%) against plant pathogens.

Bacterial Strain	Standard*	PCFE	BSDZNPs	BSDZNPs	BSDZNPs	BSDZNPs
	(10 µL)	(10 µL)	(2 µL)	(4 μL)	(6 µL)	(10 µL)
X. citri	14.06±0.08	6.50±0.01	3.04±0.09	6.03±0.02	10.00±0.06	13.03±0.03
P. syringae	18.05±0.09	7.01±0.03	5.05±0.02	9.02±0.07	14.00±0.07	19.05±0.08
Fungal cultures	Standard** (10 µL)	PCFE (10 μL)	BSDZNPs (5 μL)	BSDZNPs (10 µL)	BSDZNPs (15 µL)	BSDZNPs (20 µL)
A. niger	18.02±0.09	12.02±0.09	5.05±0.09	10.08±0.04	12.06±0.07	16.06±0.01
A. flavus	25.09±0.08	13.11±0.02	5.00±0.00	9.01±0.09	14.02±0.09	20.02±0.09
A. fumigatus	16.08±0.01	6.01±0.07	2.02±0.09	6.20±0.02	9.07±0.00	16.02±0.09
A. terreus	13.21±0.09	8.03±0.03	3.40±0.01	6.01±0.08	10.08±0.02	13.01±0.05
P. chrysogenum	23.06±0.02	6.02±0.09	4.00±0.01	6.20±0.08	13.20±0.04	28.07±0.02
F. solani	18.06±0.03	9.01±0.02	3.90±0.08	9.09±0.01	13.09±0.07	16.09±0.01
L. theobromae	19.08±0.05	11.04±0.02	5.03±0.01	7.02±0.04	13.00±0.03	16.00±0.01

(* Ampicillin, ** Amphotericin B)



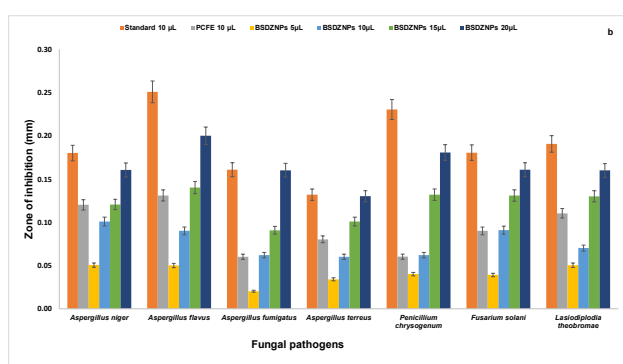
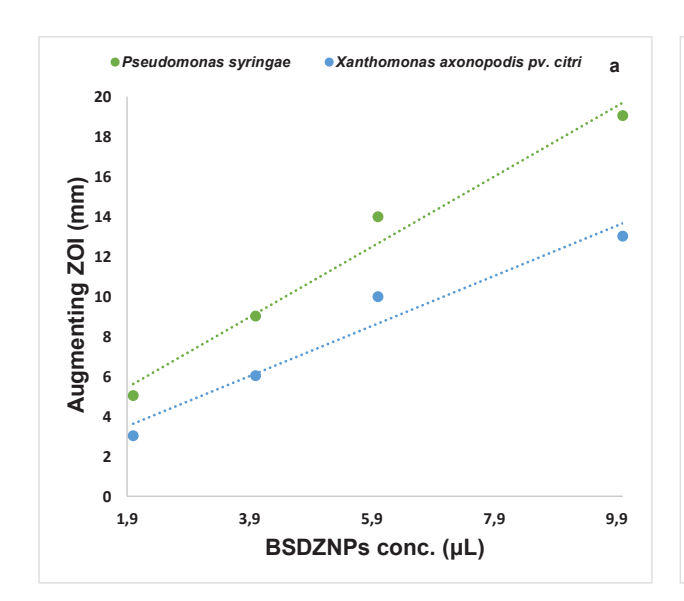


Figure 8: Comparative in vitro antimicrobial efficacy of biogenic silver doped ZnO nanoparticles (2.0% doped) derived from P. cerasifera against (a) bacterial; (b) fungal pathogens.

mutation in the host microbial cell. Though, very meagre and hardscrabble antimicrobial activity has been reported for chemically synthesized ZnO [72], green synthesized ZnO [73-75], chemically doped ZnO NPs [76-79] but studies comprising phytosynthetic BSDZNPs have never been reported. Thus in present investigation the

antibacterial and antifungal activity of BSDZNPs were determined for nine pathogenic strains of biomedical and agricultural significance i.e. X. citri, P. syringae, A. niger, A. flavus, A. fumigatus, A. terreus, P. chrysogenum, F. solani and L. theobromae by standard Kirby-Bauer disc diffusion assay (Table 2, Figure 8). Plant pathogens are responsible for causing calamitous diseases in leaves, stem, fruit, flowers etc. in important crops like wheat, rice, cotton, sugarcane, fruits and vegetable, cereals etc. PCFE produced considerable zones of inhibition against all tested microbes which makes it a suitable candidate for bioprospecting. Silver is known for its bactericidal and fungicidal efficaciousness among all metals in addition to its least toxicity towards faunal cells. Silver transmetallic conversion to nano regime is associated with augmented antimicrobial potency, thus Ag doped ZnO nanoparticles also expressed good inhibition zones. BSDZNPs expressed higher clearance zones for P. syringae than X. citri, while in case of fungal pathogens, the highest activity was obtained for A. flavus and A. terreus was least inhibited. The inhibition of BSDZNPs exceeded standard drug for P. chrysogenum while for other microbes it was comparable to it. The growth inhibition activity at equal dose of standard drug and BSDZNPs shows BSDZNPs to be the green alternative for available drugs. All microorganisms produced no zone of inhibition for Ag salt solution (not shown in table) due to their resistance towards Ag but were effectively controlled by BSDZNPs.



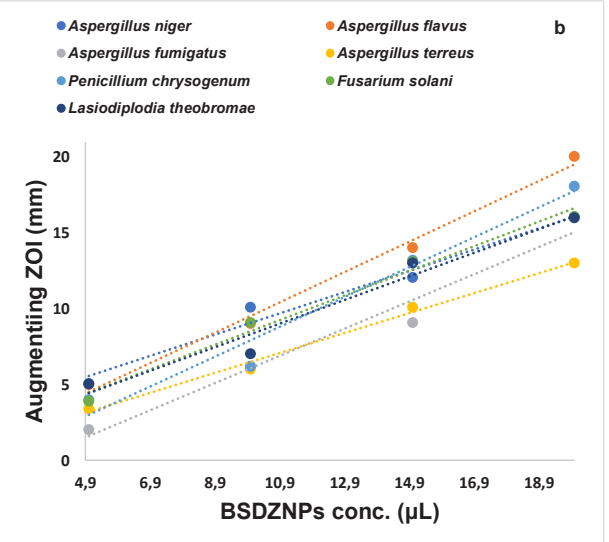


Figure 9 Augmented zones of inhibition resulting from increased concentration (μ L) of biogenic silver doped ZnO nanoparticles (2.0% doped) (a) bacterial; (b) fungal pathogens.

Positive correlation was observed between the BSDZNPs concentration (µL) and zone of inhibition (mm). BSDZNPs inhibited the growth of bacterial and fungal pathogens in dose dependent manner (Figure 9a,b). Antimicrobial activity shows the susceptibility of all significant microbes towards BSDZNPs. Such inhibition can be considered as the synergistic effect of inherent toxicity possessed by Ag and ZnO NPs. Ag has antimicrobial potential via enzyme mediated respiratory chain disruption [80] while the increased surface area of ZnO with surface defects in crystal phase is responsible for elevated production of H₂O₂ [81, 82] as well as Zn²⁺ ions are being dissolved leading to microbial cell lysis. Dose dependence of microbial inhibition is governed by incrementinsilverwhichresultsinanenhancedattachment to microbial cell. Thus, the enhanced performance of BSDZPs over commercial ZnO is advantageous and in compliance with all principles of green chemistry [83]. The tested gram negative strains were effectively inhibited by BSDZNPs due to their weaker peptidoglycan layer and effective electrostatic bonding between BSDZNPs and test microbes thus inducing physicochemical changes in bacterial cells [84-87]. However, nano fungicidal efficacy is because of disintegration of thiol groups found in fungal cell wall thus forming compounds with zero solubility. Such alterations causes rupture in membrane enzymatic and lipid components thus inducing cellular lytic reactions [55]. Inhibition zones obtained for BSDZNPs are comparable with the standard antibiotic drugs thus indicating their conversion into green nano bactericide and nano fungicide for wiping out all pathogens that pose

great harm to human health and result in loss of valuable crops every year. By utilization of green nano fungicide, the need for chemical agents [88-93] will be nullified and effective inhibition rates will be obtained.

4 Conclusions

Ag doped ZnO nanoparticles can be reduced and stabilized by the phytochemicals found in P. cerasifera fruit extract through novel, unprecedented and eco-friendly biogenic route. The compositional, crystalline, morphological and optical characteristics confirms the suitability of BSDZNPs as functional nano biomaterials. Biogenic Ag doped ZnO nanoparticles expressed the rough surface morphology with size ranges reducing with an increase in dopant percentage. Hexagonal wurtzite crystals with average crystal size of 2.99 nm are obtained. The band gap reduction from 3.3.7 eV to 2.81 eV upon Ag doping augments the photocatalytic potential. Ag doped ZnO nanoparticles are practically efficient photo catalysts that can photodegrade organic pollutants like Methyl Orange, Safranine O and Rhodamine B in short duration. Remarkable degradation percentages obtained for Ag doped ZnO nanoparticles promotes its utilization in environmental remediation. The dose dependent in vitro bio activity of Ag doped ZnO nanoparticles against bacterial and fungal pathogens makes it a green nano bactericide and fungicide against resistant microbes.

Conflict of interest: Authors state no conflict of interest.

References

- [1] Murphy C.J., Sau T.K., Gole A.M., Orendorff C.J., Gao J., Gou L., Hunyadi S.E., Li T., Anisotropic metal nanoparticles: synthesis, assembly, and optical applications. J. Phys. Chem., 2005, 109, 13857-13870.
- [2] Mishra Y.K., Chakravadhanula V.S., Hrkac V., Jebril S., Agarwal D.C., Mohapatra S., Avasthi D.K., Kienle L., Adelung R., Crystal growth behaviour in Au-ZnO nanocomposite under different annealing environments and photoswitchability. J. Appl. Phys., 2012, 112, 064308.
- [3] Chang C.W., Wu H.T., Huang S.H., Chen C.K., Un I.W., Yen T.J., Single-crystalline heterostructure of ZnO nanowire arrays on large Ag microplates and its photocatalytic activity. Acta Mater., 2013, 61, 6993-6999.
- [4] Kim H.J., Lee J.H., Highly sensitive and selective gas sensors using p-type oxide semiconductors: overview. Sens. Actuator B-Chem., 2014, 192, 607-627.
- Gopal P., Spaldin N.A., Magnetic interactions in transitionmetal-doped ZnO: An ab initio study. Phys. Rev. B., 2006, 74, 094418.
- [6] Chen C.H., Chiou S.H., Guo G.Y., Yao Y.D., Electronic structure and magnetic moments of 3d transition metal-doped ZnO. J. Magn. Magn. Mater., 2004, 282, 275-278.
- [7] Wu J.J., Tseng C.H., Photocatalytic properties of nc-Au/ZnO nanorod composites. Appl. Catal. B., 2006, 66, 51-57.
- [8] Wang R., Xin J.H., Yang Y., Liu H., Xu L., Hu J., The characteristics and photocatalytic activities of silver doped ZnO nanocrystallites. Appl. Surf. Sci., 2004, 227, 312-317.
- [9] Seery M.K., George R., Floris P., Pillai S.C., Silver doped titanium dioxide nanomaterials for enhanced visible light photocatalysis. J. Photochem. Photobiol., 2007, 189, 258-263.
- [10] Azizi S., Mohamad, R., Bahadoran A., Bayat S., Rahim R.A., Ariff A., Saad W.Z., Effect of annealing temperature on antimicrobial and structural properties of bio-synthesized zinc oxide nanoparticles using flower extract of Anchusa italica. J. Photochem. Photobiol., 2016, 161, 441-449.
- [11] Nava O.J., Luque P.A., Gómez-Gutiérrez C.M., Vilchis-Nestor A.R., Castro-Beltrán A., Mota-González M.L., Olivas A., Influence of Camellia sinensis extract on Zinc Oxide nanoparticle green synthesis. J. Mol. Struct., 2017, 1134, 121-125.
- [12] Bhuyan T., Mishra K., Khanuja M., Prasad R., Varma A., Biosynthesis of zinc oxide nanoparticles from Azadirachta indica for antibacterial and photocatalytic applications. Mater. Sci. Semicond. Process., 2015, 32, 55-61.
- [13] Govindarajan M., Rajeswary M., Hoti S.L., Murugan K., Kovendan K., Arivoli S., Benelli G., Clerodendrum chinensemediated biofabrication of silver nanoparticles: mosquitocidal potential and acute toxicity against non-target aquatic organisms. J. Asia. Pac. Entomol., 2016, 19, 51-58.
- [14] Jinu U., Jayalakshmi N., Anbu A.S., Mahendran D., Sahi S., Venkatachalam P., Biofabrication of cubic phase silver nanoparticles loaded with phytochemicals from Solanum nigrum leaf extracts for potential antibacterial, antibiofilm and antioxidant activities against MDR human pathogens. J. Cluster. Sci., 2017, 28, 489-505.
- [15] Saratale R.G., Benelli G., Kumar G., Kim D.S., Saratale G.D., Bio-fabrication of silver nanoparticles using the leaf extract of

- an ancient herbal medicine, dandelion (Taraxacum officinale), evaluation of their antioxidant, anticancer potential, and antimicrobial activity against phytopathogens. Env. Sci. Poll. Res., 2017, 1-5.
- [16] Chequer F.M.D., de Paula Venâncio V., Bianchi M.D.L.P., Antunes L.M.G., Genotoxic and mutagenic effects of erythrosine B, a xanthene food dye, on HepG2 cells. Food Chem. Toxicol., 2012, 50, 3447-3451.
- [17] Jiang D., Tang B., Guo H., Xu W., Xu S., Halide Ions Sensing in Water via Silver Nanoprism Self-Assembled Chips. Sci. Adv. Mater., 2013, 5, 1105-1110.
- [18] Liang Y., Guo N., Li L., Li R., Ji G., Gan S., Fabrication of porous 3D flower-like Ag/ZnO heterostructure composites with enhanced photocatalytic performance. Appl. Surf. Sci., 2013, 332, 32-39.
- [19] Ismail A.A., Facile synthesis of mesoporous Ag-loaded TiO. thin film and its photocatalytic properties. Micro. Meso. Mater., 2012, 149, 69-75.
- [20] Goei R., Lim T.T., Ag-decorated TiO, photocatalytic membrane with hierarchical architecture: Photocatalytic and anti-bacterial activities. Water Res., 2014, 59, 207-218.
- [21] Ullah R., Dutta J., Photocatalytic degradation of organic dyes with manganese-doped ZnO nanoparticles. J. Hazard. Mater., 2008, 156, 194-200.
- [22] Karunakaran C., Rajeswari V., Gomathisankar P., Antibacterial and photocatalytic activities of sonochemically prepared ZnO and Ag-ZnO. J. Alloy Comp., 2010, 508, 587-591.
- [23] Subash B., Krishnakumar B., Velmurugan R., Swaminathan M., Shanthi M., Synthesis of Ce co-doped Ag-ZnO photocatalyst with excellent performance for NBB dye degradation under natural sunlight illumination. Catal. Sci. Technol., 2012, 2, 2319-2326.
- [24] Georgekutty R., Seery M.K., Pillai S.C., A highly efficient Ag-ZnO photocatalyst: synthesis, properties, and mechanism. J. Phys. Chem. C., 2008, 112, 13563-13570.
- [25] Singh R., Barman P.B., Sharma D., Synthesis, structural and optical properties of Ag doped ZnO nanoparticles with enhanced photocatalytic properties by photo degradation of organic dyes. J. Mater. Sci. Mater. Electron., 2017, 28, 5705-
- [26] Hsu M.H., Chang C.J., Ag-doped ZnO nanorods coated metal wire meshes as hierarchical photocatalysts with high visiblelight driven photoactivity and photostability. J. Hazard. Mater., 2014, 278, 444-453.
- [27] Paul K.K., Ghosh R., Giri P.K., Mechanism of strong visible light photocatalysis by Ag2O-nanoparticle decorated monoclinic TiO₂ (B) porous nanorods. Nanotech., 2016, 27, 315703.
- [28] Zhang D., Photocatalytic oxidation of organic dyes with nanostructured zinc dioxide modified with silver metals. Russ. J. Phys. Chem., 2011, 85, 1416-1422.
- [29] Bechambi O., Chalbi M., Najjar W., Sayadi S., Photocatalytic activity of ZnO doped with Ag on the degradation of endocrine disrupting under UV irradiation and the investigation of its antibacterial activity. Appl. Surf. Sci., 2015, 347, 414-420.
- [30] Shokri M., Isapour G., Hosseini M.G., Zarbpoor Q., Enhanced Photocatalytic activity of Ag Doped ZnO nanorods for degradation of an Azo Dye. Water Envir. Res., 2016, 88, 2001-2007.

- [31] Kaur A., Ibhadon A.O., Kansal S.K., Photocatalytic degradation of ketorolac tromethamine (KTC) using Ag-doped ZnO microplates. J. Mater. Sci., 2017, 52, 5256-5267.
- [32] Blazquez J., Oliver A., Gómez-Gómez J.M., Mutation and evolution of antibiotic resistance: antibiotics as promoters of antibiotic resistance? Current drug targets., 2002, 3, 345-349.
- [33] Jaffri S.B., Ahmad K.S., Prunus cerasifera Ehrh. fabricated ZnO nano falcates and its photocatalytic and dose dependent in vitro bio-activity. Open Chem., 2018, 16, 141-154.
- [34] Abinaya C., Mayandi J., Osborne J., Frost M., Ekstrum C., Pearce J.M., Inhibition of growth of S. epidermidis by hydrothermally synthesized ZnO nanoplates. Mater. Res. Exp., 2017, 4, 075401.
- [35] Abinaya C., Marikkannan M., Manikandan M., Mayandi J., Suresh P., Shanmugaiah V., Pearce J.M., Structural and optical characterization and efficacy of hydrothermal synthesized Cu and Ag doped zinc oxide nanoplate bactericides. Mater. Chem. Phys., 2016, 184, 172-182.
- [36] Lam S.M., Quek J.A., Sin J.C., Mechanistic investigation of visible light responsive Ag/ZnO micro/nanoflowers for enhanced photocatalytic performance and antibacterial activity. J. Photochem. Photobiol., 2018, 353, 171-184.
- [37] Kumar V., Prakash J., Singh J.P., Chae K.H., Swart C., Ntwaeaborwa O.M., Dutta V., Role of silver doping on the defects related photoluminescence and antibacterial behaviour of zinc oxide nanoparticles. Colloids Surf. B., 2017, 159, 191-199.
- [38] Chen Y., Tse W.H., Chen L., Zhang J., Ag nanoparticlesdecorated ZnO nanorod array on a mechanical flexible substrate with enhanced optical and antimicrobial properties. Nano. Res. Let., 2015, 10, 1-8.
- [39] Ravichandran K., Sathish P., Snega S., Karthika K., Rajkumar P.V., Subha K., Sakthivel B., Improving the antibacterial efficiency of ZnO nanopowders through simultaneous anionic (F) and cationic (Ag) doping. Powder Technol., 2015, 274, 250-257.
- [40] Nagaraju G., Prashanth S.A., Shastri M., Yathish K.V., Anupama C., Rangappa D., Electrochemical heavy metal detection, photocatalytic, photoluminescence, biodiesel production and antibacterial activities of Ag-ZnO nanomaterial. Mat. Res. Bull., 2017, 94, 54-63.
- [41] Talari M.K., Majeed A.B.A., Tripathi D.K., Tripathy M., Synthesis, characterization and antimicrobial investigation of mechanochemically processed silver doped ZnO nanoparticles. Chem. Pharma. Bull., 2012, 60, 818-824.
- [42] Kaviya S., Prasad E., Biogenic synthesis of ZnO-Ag nano custard apples for efficient photocatalytic degradation of methylene blue by sunlight irradiation. RSC Adv., 2015, 5, 17179-171785.
- [43] Ajitha B., Reddy Y.A., Reddy P.S., Biogenic nano-scale silver particles by Tephrosia purpurea leaf extract and their inborn antimicrobial activity. Spectrochim. Acta. Mol. Bio., 2014, 121,
- [44] Al-Hadeethi Y., Umar A., Ibrahim A.A., Al-Heniti S.H., Kumar R., Baskoutas S., Raffah B.M., Synthesis, characterization and acetone gas sensing applications of Ag-doped ZnO nanoneedles. Ceram. Int., 2017, 43, 6765-6770.
- [45] Umar A., Lee J.H., Kumar R., Al-Dossary O., Highly Sensitive Ethanol Gas Sensors Based on Ag-Doped ZnO Nanocones. Nanosci. Nanotechnol. Lett., 2016, 8, 241-246.

- [46] Türkyılmaz Ş.Ş., Güy N., Özacar M., Photocatalytic efficiencies of Ni, Mn, Fe and Ag doped ZnO nanostructures synthesized by hydrothermal method: The synergistic/antagonistic effect between ZnO and metals. J. Photochem. Photobiol., 2017, 341, 39-50.
- [47] Murtaza G., Ahmad R., Rashid M.S., Hassan M., Hussnain A., Khan M.A., Riaz S., Structural and magnetic studies on Zr doped ZnO diluted magnetic semiconductor. Curr. Appl. Phys., 2014, 14, 176-181.
- [48] Zhang L., Du L., Yu X., Tan S., Cai X., Yang P., Mai W., Significantly enhanced photocatalytic activities and charge separation mechanism of Pd-decorated ZnO-graphene oxide nanocomposites. ACS Appl. Mater. Interfaces., 2014, 6, 3623-
- [49] Zhai H., Wang L., Han D., Wang H., Wang J., Liu X., Yang J., Facile one-step synthesis and photoluminescence properties of Ag-ZnO core-shell structure. J. Alloys. Compd., 2014, 600, 146-150.
- [50] SivaVijayakumar T., Karthikeyeni S., Vasanth S., Ganesh A., Bupesh G., Ramesh R., Subramanian P., Synthesis of silver-doped zinc oxide nanocomposite by pulse mode ultrasonication and its characterization studies. J. Nanosci., 2013. https://doi.org/10.1155/2013/785064
- [51] Singh R., Barman P.B., Sharma D., Synthesis, structural and optical properties of Ag doped ZnO nanoparticles with enhanced photocatalytic properties by photo degradation of organic dyes. J. Mater. Sci. Mater. Electron., 2017, 28, 5705-5717.
- [52] Sagadevan S., Pal K., Chowdhury Z.Z., Hoque M.E., Structural, dielectric and optical investigation of chemically synthesized Ag-doped ZnO nanoparticles composites. J. Sol-Gel Sci. Technol., 2017, 83, 394-404.
- [53] Rokesh K., Mohan S.C., Karuppuchamy S., Jothivenkatachalam K., Photo-assisted advanced oxidation processes for Rhodamine B degradation using ZnO-Ag nanocomposite materials. J. Environ. Chem. Eng., 2017. https://doi. org/10.1016/j.jece.2017.01.023
- [54] Begum N.J., Ravichandran K., Effect of source material on the transparent conducting properties of sprayed ZnO: Al thin films for solar cell applications. J. Phys. Chem. Solids., 2013, 74, 841-848.
- [55] Hosseini S.M., Sarsari I.A., Kameli P., Salamati H., Effect of Ag doping on structural, optical, and photocatalytic properties of ZnO nanoparticles. J. Alloys. Compd., 2015, 640, 408-415.
- [56] Karyaoui M., Mhamdi A., Kaouach H., Labidi A., Boukhachem A., Boubaker K., Chtourou R., Some physical investigations on silver-doped ZnO sprayed thin films. Mater. Sci. Semicond. Process., 2015, 30, 255-262.
- [57] Mohammad A., Kapoor K., Mobin S.M., Improved Photocatalytic Degradation of Organic Dyes by ZnO-Nanoflowers. ChemistrySelect., 2016, 1, 3483-3490.
- [58] Mittal A., Kaur D., Mittal J., Applicability of waste materials bottom ash and deoiled soya—as adsorbents for the removal and recovery of a hazardous dye, brilliant green. J. Colloid. Interface Sci., 2008, 326, 8-17.
- [59] Xu J., Chang Y., Zhang Y., Ma S., Qu Y., Xu C., Effect of silver ions on the structure of ZnO and photocatalytic performance of Ag/ ZnO composites. Appl. Surf. Sci., 2008, 255, 1996-1999.
- [60] Yıldırım Ö.A., Unalan H.E., Durucan C., Highly Efficient Room Temperature Synthesis of Silver-Doped Zinc Oxide (ZnO:

- Ag) Nanoparticles: Structural, Optical, and Photocatalytic Properties. J. Am. Ceram. Soc., 2013, 96, 766-773.
- [61] Wang Z. Xue M., Huang K., Liu Z., Textile dyeing wastewater treatment. In Advances in treating textile effluent, InTech, 2011.
- [62] Horikoshi S., Hojo F., Hidaka H., Serpone N., Environmental remediation by an integrated microwave/UV illumination technique. Fate of carboxylic acids, aldehydes, alkoxycarbonyl and phenolic substrates in a microwave radiation field in the presence of TiO2 particles under UV irradiation. Env. Sci. tech., 2004, 38, 2198-2208.
- [63] Longmire M., Ogawa M., Hama Y., Kosaka N., Regino C.A., Choyke P.L. Kobayashi H., Determination of Optimal Rhodamine Flurophore for In Vivo Optical Imaging. Bioconjug Chem., 2008,
- [64] Nguyen T., Francis M.B., Practical synthetic route to functionalized rhodamine dyes. Org. let., 2003, 5, 3245-3248.
- [65] Roosta M., Ghaedi M., Asfaram A., Simultaneous ultrasonicassisted removal of malachite green and safranin O by copper nanowires loaded on activated carbon: central composite design optimization. RSC Adv., 2015, 5, 57021-5729.
- [66] Karunakaran C., Rajeswari V., Gomathisankar P., Optical, electrical, photocatalytic, and bactericidal properties of microwave synthesized nanocrystalline Ag-ZnO and ZnO. Solid. State. Sci., 2011, 13, 923-928.
- [67] Kumaresan S., Vallalperuman K., Sathishkumar S., A Novel one-step synthesis of Ag-doped ZnO nanoparticles for high performance photo-catalytic applications. J. Mater. Sci. Mater. Electron., 2017, 28, 5872-5879.
- [68] Lai Y., Meng M., Yu Y., One-step synthesis, characterizations and mechanistic study of nanosheets-constructed fluffy ZnO and Ag/ZnO spheres used for Rhodamine B photodegradation. Appl. Catal. B., 2010, 100, 491-501.
- [69] Jang Y.J., Simer C., Ohm T., Comparison of zinc oxide nanoparticles and its nano-crystalline particles on the photocatalytic degradation of methylene blue. Mater. Res. Bull., 2006, 41, 67-77.
- [70] Din M.I., Khalid R., Hussain Z., Minireview: Silver-Doped Titanium Dioxide and Silver-Doped Zinc Oxide Photocatalysts. Anal. Lett., 2017, 1-16. https://doi.org/10.1080 /00032719.2017.1363770
- [71] Hajipour M.J., Fromm K.M., Ashkarran A.A., de Aberasturi D.J., de Larramendi I.R., Rojo T., Mahmoudi M., Antibacterial properties of nanoparticles. Trends Biotechnol., 2012, 30, 499-511.
- [72] Khan S.A., Noreen F., Kanwal S., Iqbal A., Hussain G., Green synthesis of ZnO and Cu-doped ZnO nanoparticles from leaf extracts of Abutilon indicum, Clerodendrum infortunatum, Clerodendrum inerme and investigation of their biological and photocatalytic activities. Mater. Sci. Eng. C., 2017; 82, 46-59.
- [73] Malaikozhundan B., Vaseeharan B., Vijayakumar S., Pandiselvi K., Kalanjiam M.A.R., Murugan K., Benelli G., Biological therapeutics of Pongamia pinnata coated zinc oxide nanoparticles against clinically important pathogenic bacteria, fungi and MCF-7 breast cancer cells. Microb. Pathog., 2017, 104, 268-277.
- [74] Asghar M.A., Zahir E., Shahid S.M., Khan M.N., Asgher M.A., Iqbal J., Walker G., Iron, copper and silver nanoparticles: Green synthesis using green and black tea leaves extract and evaluation of antibacterial, antifungal and aflatoxin B 1

- adsorption activity. Lebenson Wiss Technol. 2017. https://doi. org/10.1016/j.lwt.2017.12.009
- [75] Jaffri S.B., Ahmad K.S., Augmented photocatalytic, antibacterial and antifungal activity of prunosynthetic silver nanoparticles. Artif. Cells. Nanomed. Biotechnol., 2017, 1-11. https://doi.org/10.1080/21691401.2017.1414826
- [76] Khan S.A., Shahid S., Jabin S., Zaman S., Sarwar M.N., Synthesis and characterization of un-doped and Copper-doped Zinc oxide nanoparticles for their optical and antibacterial studies. Dig. J. Nanomater. Biostruct., 2018, 13, 285-297.
- [77] Shahid S., Khan S.A., Ahmad W., Fatima U., Knawal S., Sizedependent Bacterial Growth Inhibition and Antibacterial Activity of Ag-doped ZnO Nanoparticles under Different Atmospheric Conditions. Indian. J. Pharm. Sci., 2018, 80, 173-
- [78] Khan S.A., Shahid S., Bashir W., Kanwal S., Iqbal A., Synthesis, characterization and evaluation of biological activities of manganese-doped zinc oxide nanoparticles. Trop. J. Pharm. Res., 2017, 16, 2331-2339.
- [79] Khan S.A., Noreen F., Kanwal S., Hussain G., Comparative synthesis, characterization of Cu-doped ZnO nanoparticles and their antioxidant, antibacterial, antifungal and photocatalytic dye degradation activities. Dig. J. Nanomater. Biostruct., 2017, 12, 877-889.
- [80] Kumar A., Vemula P.K., Ajayan P.M., John G., Silvernanoparticle-embedded antimicrobial paints based on vegetable oil. Nat. Mater., 2008, 7, 236-241.
- [81] Brett D.W., A discussion of silver as an antimicrobial agent: alleviating the confusion. Ostomy Wound Manage., 2006, 52, 34-41.
- [82] Amornpitoksuk P., Suwanboon S., Sangkanu S., Sukhoom A., Wudtipan J., Srijan K., Kaewtaro S., Synthesis, photocatalytic and antibacterial activities of ZnO particles modified by diblock copolymer. Powder Tech., 2011, 212, 432-438.
- [83] Talari M.K., Majeed A.B.A., Tripathi D.K., Tripathy M., Synthesis, characterization and antimicrobial investigation of mechanochemically processed silver doped ZnO nanoparticles. Chem. Pharm. Bull., 2012, 60, 818-824.
- [84] Sondi I., Salopek-Sondi B., Silver nanoparticles as antimicrobial agent: a case study on E. coli as a model for Gram-negative bacteria. J. Colloid. Interface Sci., 2004, 275,
- [85] Nel A.E., Mädler L., Velegol D., Xia T., Hoek E.M., Somasundaran P., Klaessig F., Castranova V., Thompson M., Understanding biophysicochemical interactions at the nanobio interface. Nat. Mater., 2009, 8, 543-557.
- [86] Su H. L., Chou C.C., Hung D.J., Lin S.H., Pao I.C., Lin J.H., Huang F.L., Dong R.X., Lin J., The disruption of bacterial membrane integrity through ROS generation induced by nanohybrids of silver and clay. J. Biomat., 2009, 30, 5979-5987.
- [87] Jaidev L.R., Narasimha G., Fungal mediated biosynthesis of silver nanoparticles, characterization and antimicrobial activity. Colloids Surf. B., 2010, 81, 430-433.
- [88] Ahmad K.S., Rashid N., Sorption-Desorption Behavior of Newly synthesized N-(1H-Benzimidazole-2 ylmethyl) Acetamide (ABNZ) on Selected Soils and its Antifungal activity. J. Chem. Soc. Pak., 2015, 37, 841-849.
- [89] Ahmad K.S., Rashid N., Nazar M.F., Tazaiyen S., Adsorption and Desorption Characteristic of Benzimidazole Based Fungicide

- Carbendazim in Pakistani Soils. J. Chem. Soc. Pak., 2013, 35,
- [90] Ahmad K.S., Pedospheric sorption investigation of sulfonyl urea herbicide Triasulfuron via regression correlation analysis in selected soils. S. Afr. J. Chem., 2017, 70, 163-170.
- [91] Ahmad K.S., Investigating the impact of soils' physicochemical composition on chlorsulfuron pedospheric sorption. Stud. U. Babes-Bol. Che., 2017, 62, 165-174.
- [92] Ahmad K.S., Rashid N., Tazaiyen S., Zakria, M., Sorption-Desorption Characteristics of Benzimidazole Based Fungicide 2-(4-fluorophenyl)-1H-benzimidazole on Physicochemical Properties of Selected Pakistani Soils. J. Chem. Soc. Pak., 2014, 36, 1189-1195.
- [93] Ahmad K.S., Green electrokinetic remediation of Thiabendazole adsorbed soils via mineralization. Agrochimica., 2017, 61, 190-205.

Supplemental Material: The online version of this article offers supplementary material (https://doi.org/10.1515/chem-2018-0060).